Gamblin et al., http://www.jcb.org/cgi/content/full/jcb.201308032/DC1

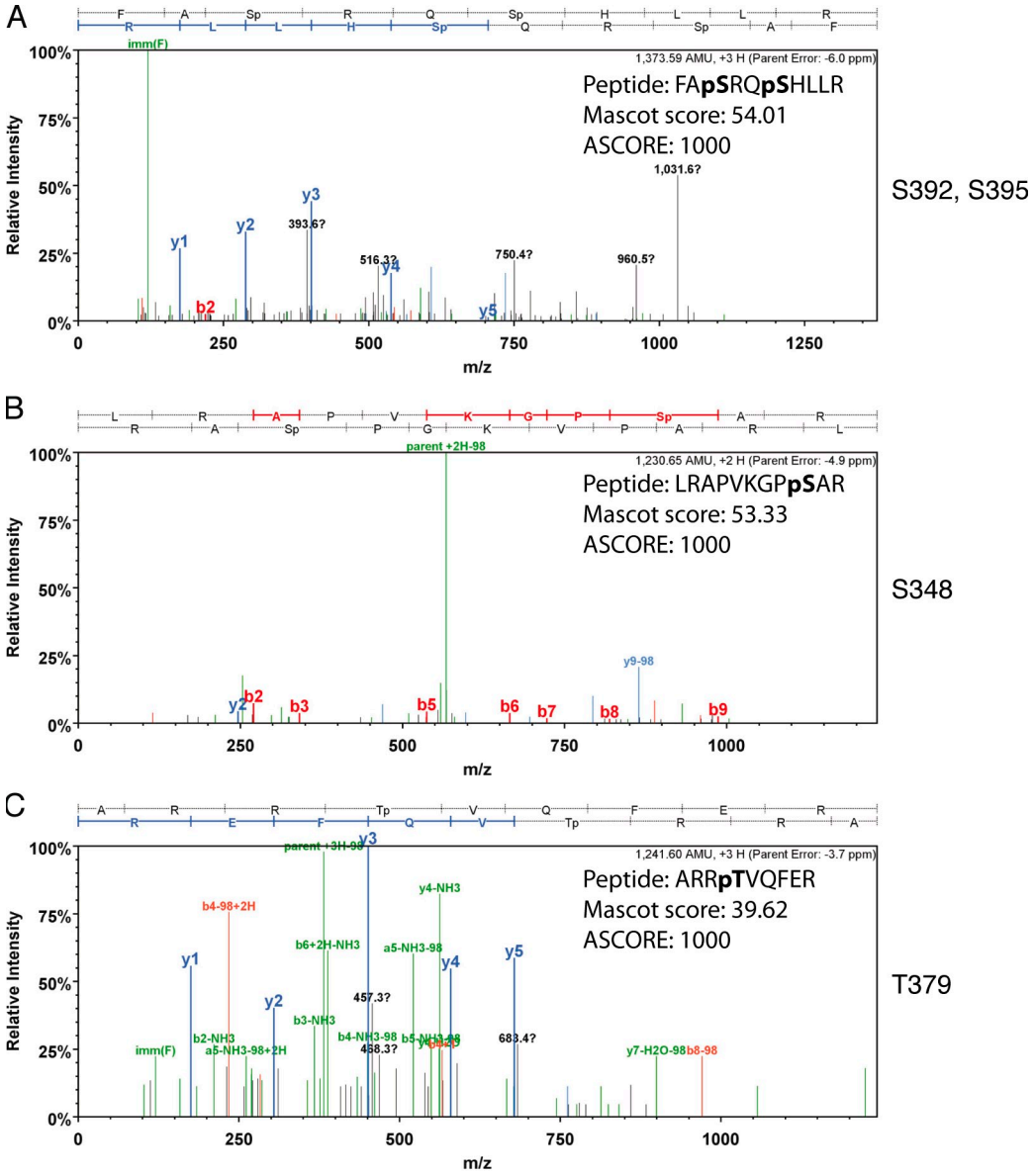

Figure S1. **Identification of aPKC phosphorylation sites in Yrt by mass spectrometry.** (A–C) Representative MS/MS spectra for phosphopeptides containing residues S392 and S395 (A), S348 (B), and T379 (C). Mascot scores for peptide identification and Ascore for site localization are both indicated within panels. A total of three peptides containing S348 was found, one peptide was found for T379, and four peptides were found for S392/S395. m/z, mass per charge; AMU , atomic mass unit.

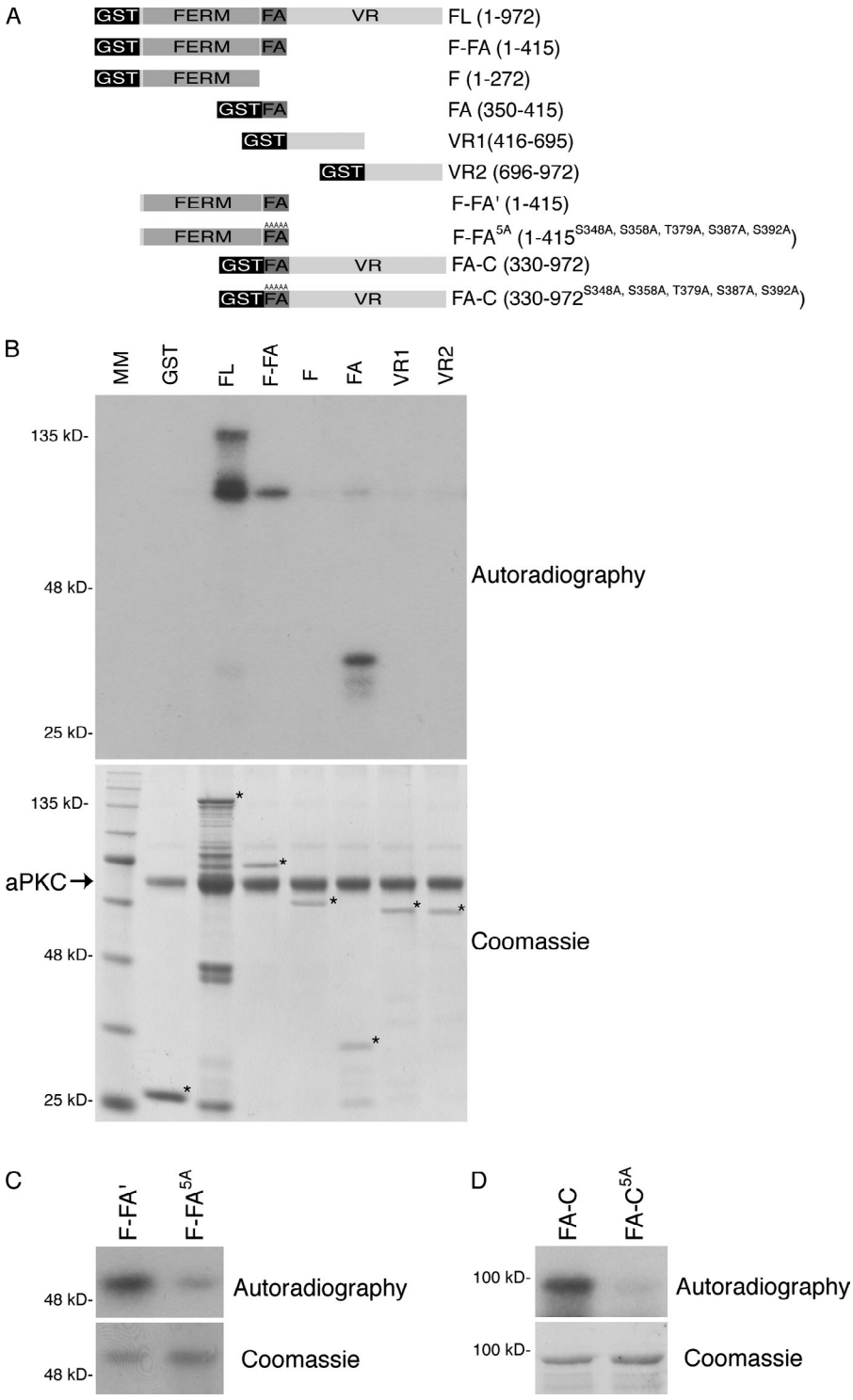

Figure S2. **The FA domain of Yrt contains most aPKC phosphorylation sites.** (A) Schematic representation of the GST fusion proteins used in B–D. Substrates used in B and D were fused to GST. In contrast, constructs used in C were not, as they were cleaved off GST using the PreScission protease. (B) Purified aPKC was incubated with GST coupled to full-length (FL) Yrt or truncations of it in the presence of radiolabeled ATP. Truncations containing the FA domain of Yrt were phosphorylated by aPKC. Coomassie blue staining shows the amount of substrate used in each sample. Asterisks mark the position of substrates. MM stands for molecular mass marker. (C and D) To test whether constructs lacking the FA domain are not phosphorylated simply because they do not bind to aPKC, we mutagenized the residues targeted by aPKC within the FA domain in the FERM-FA (F-FA) construct (C) and in a truncation containing the FA domain plus the entire C-terminal portion of Yrt (FA-C) (D). Mutation of these amino acids strongly reduced aPKC-dependent phosphorylation of both constructs. This suggests that most aPKC phosphorylation sites in Yrt are part of the FA domain. Coomassie blue staining controls the amount of substrate used in each sample. VR, variable region.

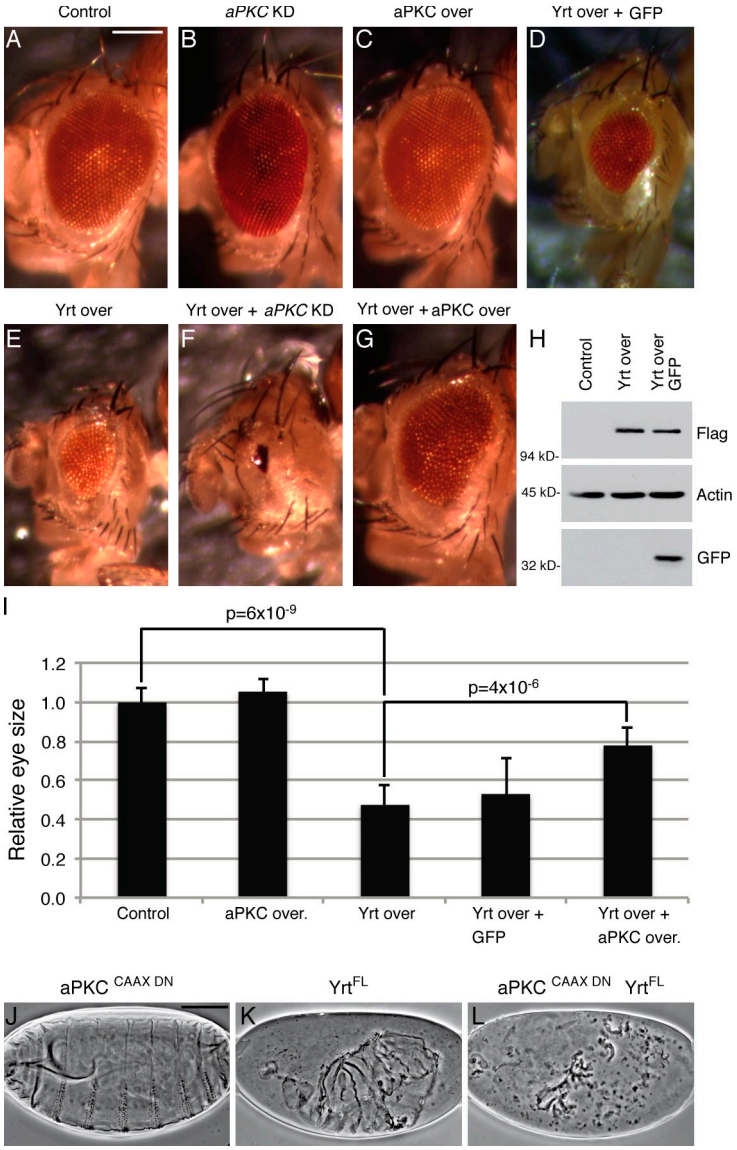

Figure S3. **aPKC limits the impact of Yrt overexpression.** (A) The panel shows a picture of a control eye. (B–G) Transgenes or shRNAs were under the control of UAS sequences and driven in the developing eye by *eyeless-GAL4*. Panels depict the eye phenotype associated with the knockdown of *aPKC* (*aPKC* KD; B), overexpression of aPKC (aPKC over; C), overexpression of Flag-Yrt and expression of GFP (Yrt over + GFP; D), overexpression of Yrt (Yrt over; E), overexpression of Flag-Yrt and knockdown of *aPKC* (Yrt over + *aPKC* KD; F), and cooverexpression of Flag-Yrt and aPKC (Yrt over + aPKC over; G). Yrt overexpression is associated with a reduction of eye size. This small eye phenotype was suppressed by overexpression of aPKC, whereas it was enhanced by *aPKC* knockdown. These results suggest that aPKC functionally represses Yrt activity in vivo. Bar, 150 μm (also applies to B–G). (H) Western blots showing that the presence of a second UAS promoter (*UAS-GFP*) had limited impact on Flag-Yrt expression. (I) The surface area of 10 eyes from 10 different flies was measured for each genotype. The mean eye size of control flies was set to 1, and the histogram shows the relative eye size for each genotype. Error bars represent standard deviation, and the statistical significance was determined using Student's analysis on log-transformed ratio. (J–L) Cuticle preparation of embryos of the following genotypes: *UAS-aPKC*$^{CAAX\ DN}$; *da-GAL4* (ubiquitous expression of a dominant-negative form of aPKC; J), *da-GAL4/UAS-Flag-yrt*^{FL} (ubiquitous expression of Flag-tagged Yrt^{FL}; K), and *UAS-aPKC*$^{CAAX\ DN}$; *da-GAL4/UAS-Flag-yrt*^{FL} (L). Bar, 100 μm (also applies to K and L).